

Investigation of Ceramic Based Composites by Using 2D Graphene Filler

Zeeshan Abbas*, Rashid Jalil, Ibtisam Riaz, Muhammad Tahir

University of Engineering and Technology, Lahore, Pakistan
Email: *zeeshanabbas7777@gmail.com

How to cite this paper: Abbas, Z., Jalil, R., Riaz, I. and Tahir, M. (2022) Investigation of Ceramic Based Composites by Using 2D Graphene Filler. *Graphene*, 11, 19-29.
<https://doi.org/10.4236/graphene.2022.112002>

Received: April 2, 2022

Accepted: April 26, 2022

Published: April 29, 2022

Copyright © 2022 by author(s) and Scientific Research Publishing Inc.
This work is licensed under the Creative Commons Attribution International License (CC BY 4.0).
<http://creativecommons.org/licenses/by/4.0/>



Open Access

Abstract

The ceramic composites of sodium bismuth titanate with reduce graphene oxide NBT/rGO of different compositions were fabricated by solid state sintering method and characterized. In this work, the graphene oxide (GO) and reduce graphene oxide (rGO) was successfully synthesized by Hummer's modified method which is confirmed by FTIR and XRD results. The reduce graphene oxide used as 2D filler in piezoelectric ceramic material. The crystalline structure of NBT/rGO composite was confirmed by X-ray diffraction with rhombohedral symmetry. The dispersion of rGO in the ceramic can be detect by the optical microcopy images. The electrical conductivity of sodium bismuth titanate shows increase at higher values of frequency and conductivity nanocomposites of different wt% were start decreases up to certain value of frequency. The broadening of peaks in frequency explicit plots of electrical conductivity with the help of LCR Meter (Impedance Capacitance and Resistance). The crystalline size of reduced graphene oxide and NBT is calculated by Scherrer's formula of XRD peaks.

Keywords

Sodium Bismuth Titanate, Graphene Oxide, Reduce Graphene Oxide, Electrical Conductivity

1. Introduction

The Sodium Bismuth Titanate (NBT) belongs to dielectric material family and it is new class of dielectrics. It is a lead-free piezoelectric ceramic and it is studied widely because of its high dielectric constant [1] [2]. The NBT material covers large range of temperature and because of its large temperature range stability it is best suited for use in oil and gas sector, automotive and military applications. Structure of BNT is an ABO₃ distorted perovskite with a rhombohedral R3c

crystal symmetry at ambient temperature. The basic perovskite formula (ABO₃) of NBT is $(\text{Bi}_{0.5}\text{Na}_{0.5})\text{TiO}_3$. The (ABO₃) crystal structure for NBT consider as the sodium and bismuth cations are present at the corners of unit cell, cations of titanium go to center of oxygen octahedral while oxygen cations move to faces of cubic cell [2] [3] [4].

The NBT is considered as a fantastic contender of lead-free piezoelectric ceramics for it has rhombohedral symmetry with $a = 3.891\text{Å}$ and $\alpha = 89^{\circ}36'$ at normal temperature. Where NBT becomes very interesting ferroelectric material due to its large polarization $P_r = 38\mu\text{C}/\text{cm}^2$ and large coercive effect $E_c = 73\text{kV}/\text{cm}$. In NBT structure A-sites are occupied due to Bi^{3+} and Na^+ and B-sites are occupied due to Ti^{4+} [2] [5].

Graphene is a monoatomic layered carbon's material that having single atomic thickness, smooth, honeycomb like structure and bound firmly. Graphene discovery had a great influence upon the research that reflected back by the published papers all over the world and still research is carried out. We may say that fullerenes (0D), nanotube (1D), and piled graphite (3D) are all the different structures of grapheme [6] [7]. The simplest way to obtain graphene sheet or graphene layers is stacking method (by mechanical exfoliation method) [8]. Carbon has two well-known crystals diamond and graphite that are present in bulk form and shows their unique symmetry and properties like mechanical strength [9]. These two forms of carbon are used for different application that reflects by their bonding. In graphene carbon-carbon bonds occurs due to the positioning of electrons of $2p_x$ and $2p_y$ with $2s$ orbitals. These orbitals offer ascent to steady and localized σ bonds [10]. The graphene has very large electrical conductivity because its bandgap between conduction band and valence band is zero and also known as semimetal [11] [12] [13].

2. Experimental

2.1. GO Synthesis

Initially 6 g graphite powder was purified. 60 ml Hydrofluoric acid (HF) was added to the 10 g graphite powder and magnetically stirred four one hour. Then deionized water (DIW) was added to it and washed until pH neutralized to 7. At 100°C , graphite sample was dried by using magnetic stirrer. Now graphite was purified so modified hummers method could start for the synthesis of graphene oxide. 36 g of potassium permanganate (KMnO_4) and 6 g of graphite powder were stirred for mix-up; for several minutes. Another solution was prepared by mixing 720 ml sulfuric acid (H_2SO_4) with 80 ml phosphoric acid (H_3PO_4) and stirred for several minutes. Now add the solution of (KMnO_4 + Graphite) in solution of (H_2SO_4 + H_3PO_4) slowly. After stirring 12 hours the solution changes its color to dark green. Then 800 ml deionized water (DIW) and 10 ml hydrogen peroxide (H_2O_2) added to GO solution and stirring it 10 minutes for the removal of excess KMnO_4 . Now reducing the temperature of occurred exothermic reaction by ice bathing. Now for neutralization of GO solution it was washed several

times with HCl and DIW. Washing of solution continue until its PH becomes 7 or neutralized. To obtain graphene oxide (GO) powder the washed graphene oxide solution was dried at 70 °C for 24 hours by using oven [14] [15] [16].

2.2. rGO Preparation

For Reduction of graphene oxide (GO) we dispersed graphene oxide powder into DI water at the rate of 0.2 mg/ml. The solutions of graphene oxide (GO) were sonicated in an ultrasound bath for 2 hours. Then the dispersed solution of GO was placed into autoclave and heat at 180 °C for 4 hours [17]. The internal pressure of 400 KPa was applied into autoclave. After heating, the autoclave was cool down to ambient temperature naturally [18]. The sample of reduce graphene oxide was collected and washed with DI water to dry at room temperature overnight to obtain powder of reduce graphene (rGO) [17] [19].

2.3. Preparation of NBT Composites

The ceramic based composite was prepared with two different powders. The 1st one is Sodium bismuth titanate (NBT), which was added as matrix and the 2nd one was reduce graphene oxide (rGO) which used as filler in the martix. The milling of materials was done for four hours at 200 rev/mint using zirconia balls as grinding media in Teflon jars in a planetary milling. Ethanol was used as a dispersant. Ball milled powders were heated at 70 °C for one day. Drying process was done for the removal ethanol [3] [20] [21] [22].

We prepare four sample with different weight percentage (%) of reduce graphene in NBT (0.5%, 1%, 3%, 5% in 3 g of NBT). These powders were mixed by ball milling technique. Then the powder of composite is collected by filtration [23].

Pressing is the technique of fabricating ceramic components by the compaction of powder in a metal die set. Then the sample were placed between the platen 1 & 2 in a uniaxial hydraulic press for the formation of pellets of weight of 0.5 g [24]. Each sample placed under hydraulic press for 15 mints and pressure buildup of 3000-pound square per meter (PSM). Then the pellets were baked and sintered under high temperature of 1075 °C for 2 hours in a box furnace [4] [22] [25] [26].

3. Results and Discussion

3.1. Results

3.1.1. FTIR of GO and rGO

The FTIR is preferred because it provides all information about functional groups which attached with sample (**Figure 1**). We use solid samples for FTIR. The FTIR spectra show broad and deep peaks at different range. Firstly, the peaks of GO appear between 3723 - 3071 cm^{-1} that shows hydroxyl group (O-H stretching) which is due water absorption. The spectra at 1564 cm^{-1} and 1358 cm^{-1} represent C=C stretching and C-H group. The peaks at 1228 cm^{-1} and 1048 cm^{-1} represent C-O stretching and CO-O-CO stretch in anhydride. On the other

hand, rGO peaks at 3833 and 3727 cm^{-1} shows O-H stretching. The spectra at 1649 cm^{-1} and 1546 cm^{-1} gives C=C stretching and N-O stretching [27] [28].

3.1.2. FTIR of rGO/NBT Composites

Now this given graph (Figure 2) belongs to NBT with different concentration 1%, 3% and 5%. The peaks of rGO in the NBT material can be easily detected. The peak at 998 cm^{-1} shifted towards 1008 cm^{-1} can be seen clearly as we increase

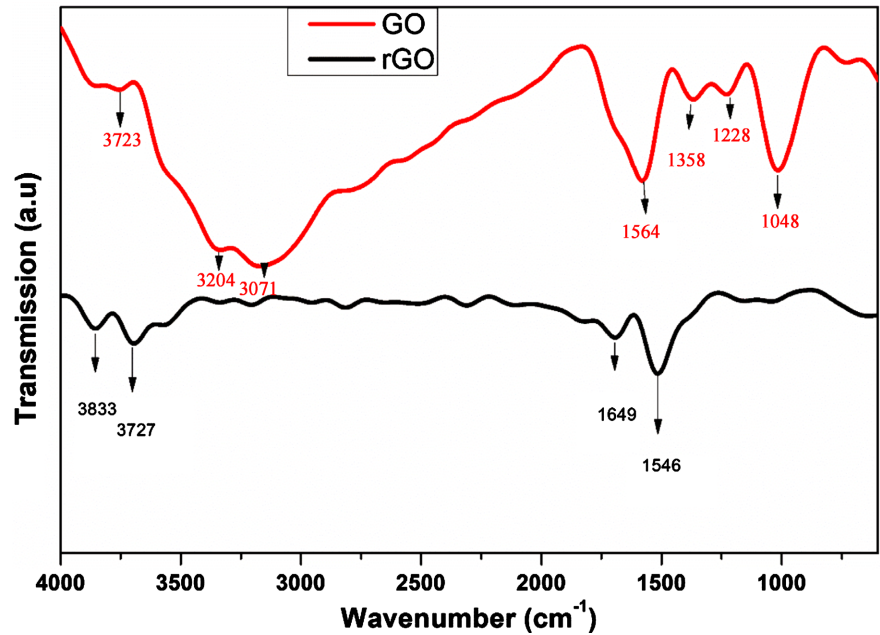


Figure 1. FTIR of graphene oxide and reduce graphene oxide.

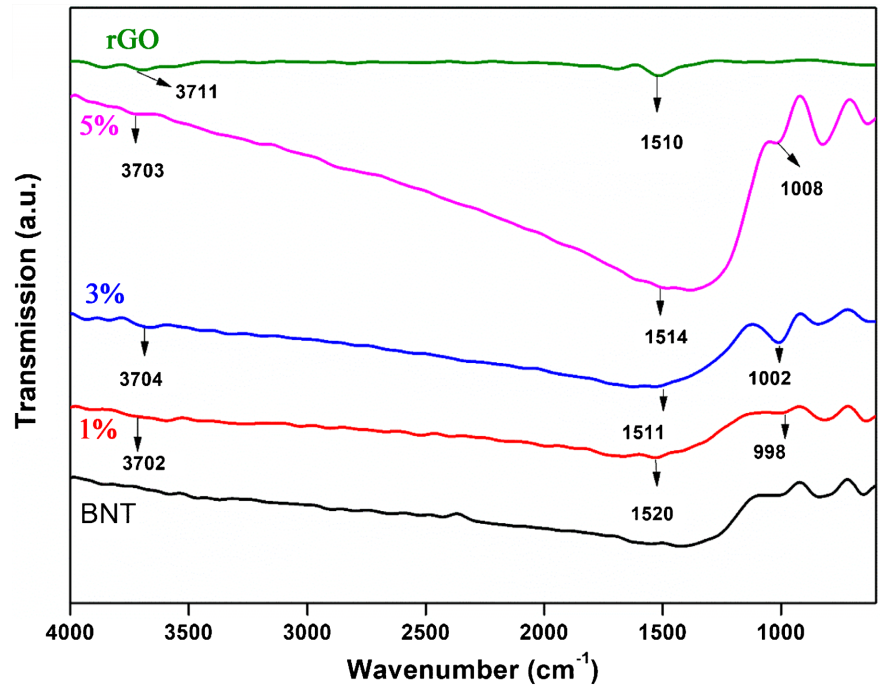


Figure 2. FTIR of rGO, NBT, 1%, 3% and 5% of rGO in NBT.

the weight percentage of rGO in the NBT. The peak at 1520 also been seen increased as the concentration of reduce graphene increased. Last peak in the graph at the range 3700 cm^{-1} is also due to rGO which shows O-H stretching of hydroxyl group [23].

3.2. Optical Analysis

NBT/rGO ceramic composites were examined under optical microscopy. This technique is simplest and easy to find reduce graphene in sodium bismuth titanate structure. The dispersion of rGO in the ceramic can be detected by the optical microcopy images [11] [29]. The optical images of ceramic composites are showed in the given **Figure 3**.

Figure 3(a) shows image of pure NBT and **Figures 3(b)-(d)** represent 1%, 3% and 5% concentration of reduce graphene in the NBT ceramic material at $50\times$ magnification. In images of ceramic composites, shiny material which is graphene distributed over the NBT matrix representing that the reduce graphene oxide filler was successfully dispersed in the NBT. In these optical image's spots on the surface of NBT represent the concentration of rGO where BNT ceramic is matrix and rGO is 2D filler. We can see rGO clearly as we increase the percentage of concentration in matrix [30].

3.3. LCR Meter Analysis

In this work sample is attached to probs of the LCR meter and placed in an electrical heater and temperature increases in discrete manners up to 500°C . The sample is coated by silver paint and LCR is done at frequency between 100 Hz to 1 MHz at different temperature starting from 25°C with a difference of 25°C for each reading [10]. The capacitance and resistance of material are obtained by the

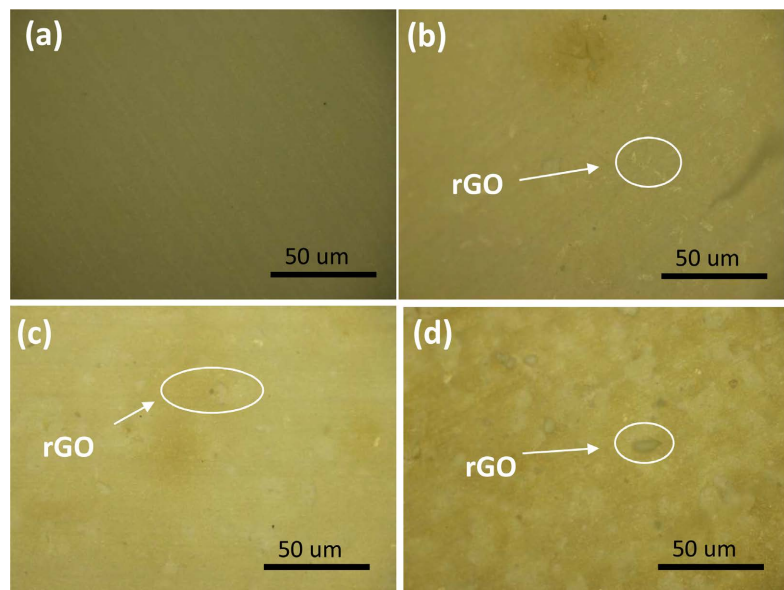


Figure 3. Optical images (a) shows image of pure NBT and the figures (b), (c) and (d) represent 1%, 3% and 5% concentration of reduce graphene in the NBT.

LCR meter [31]. We can calculate the conductivity with the given formula;

$$R = \rho \frac{L}{A}$$

Now we can explain the electrical conductivity of NBT ceramic and rGO/NBT composite which is doped by reduced graphene oxide rGO with different wt% (1%, 3% & 5%). As the concentration of rGO increases in the sample it shows decrease in electrical conductivity. We draw a graph of LCR meter between frequency and conductivity with sodium bismuth titanate doping by reduced graphene oxide with different weight percentage (Figure 4).

Firstly, we analysis electrical conductivity at (200°C, 300°C, 400°C & 500°C) which shows decrease in the conductivity as temperature from 200°C to 500°C at different values as shown in the graphs of NBT ceramic and rGO/NBT composite of different wt% (1%, 3% & 5%) [24] [32]. The impedance spectroscopy shows that conductivity of ceramic composite decreases as the concentration of rGO increases in the composite.

This shows that when rGO was added to piezoelectric ceramic, it become

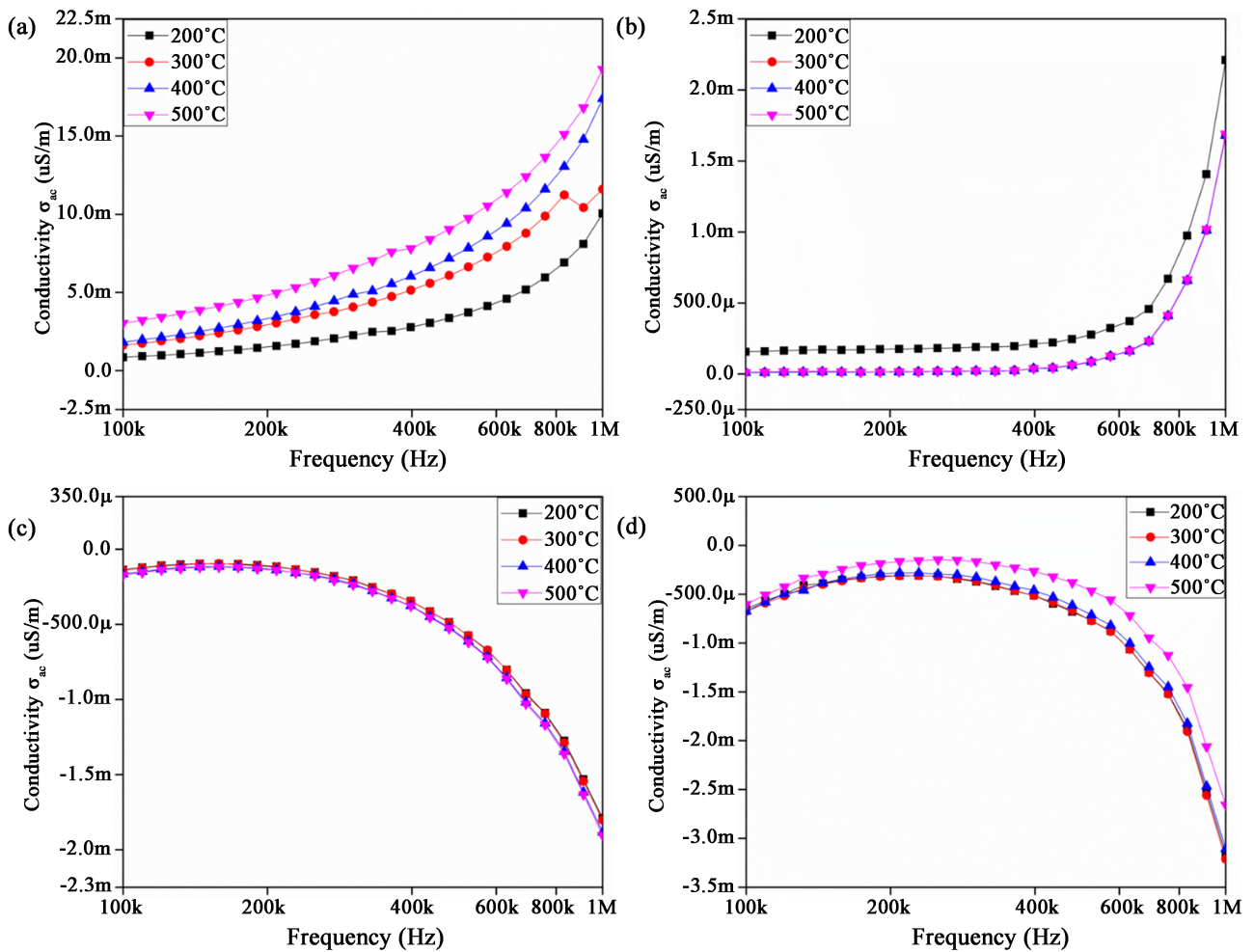


Figure 4. LCR meter electrical conductivity analysis of (a) pure NBT (b) 1% of rGO in NBT (c) 3% of rGO in NBT (d) 5% of rGO in NBT.

semimetal composite of zero band gap [33]. The value of electrical conductivity of conducting composite shows decreases as wt% of filler increases in the composite in **Table 1**. The LCR Meter show results that conductivity of ceramic composite decreases at 1 MHz as the concentration of rGO increases in the composite. This shows that when rGO was added to NBT, it become semimetal composite of zero band gap. The electrical conductivity of conducting composite decreases at high frequency as wt% of filler increases in the composite.

3.4.1. XRD of rGO

Now XRD pattern of reduce graphene oxide is given in **Figure 5** that provides information about the planes. The main peak appears at 26.608 (a.u) where two other peaks also appear at 34.98 and 42.52 (a.u) [27].

The crystalline size of rGO is calculated by the Scherrer's formula which is given in the above **Table 2**. The crystalline size at 26.60 (a.u) is 14.22 nm, where the size of crystalline at 34.98 and 42.52 (a.u) are 6.26 and 3.94 nm respectively. The average crystalline size of NBT is taken as 8.14 nm [28].

3.4.2. XRD of NBT

Now the sodium bismuth titanate (NBT) is a piezoelectric material with the help

Table 1. Calculation of electrical conductivity by LCR meter.

Temperature	Conductivity of NBT	Conductivity of 1% rGO	Conductivity of 3% rGO	Conductivity of 5% rGO
200	0.01005	0.00221	-0.00179	-0.00317
300	0.0116	0.00168	-0.00180	-0.00321
400	0.0174	0.00168	-0.00188	-0.00311
500	0.01928	0.00168	-0.00191	-0.00226

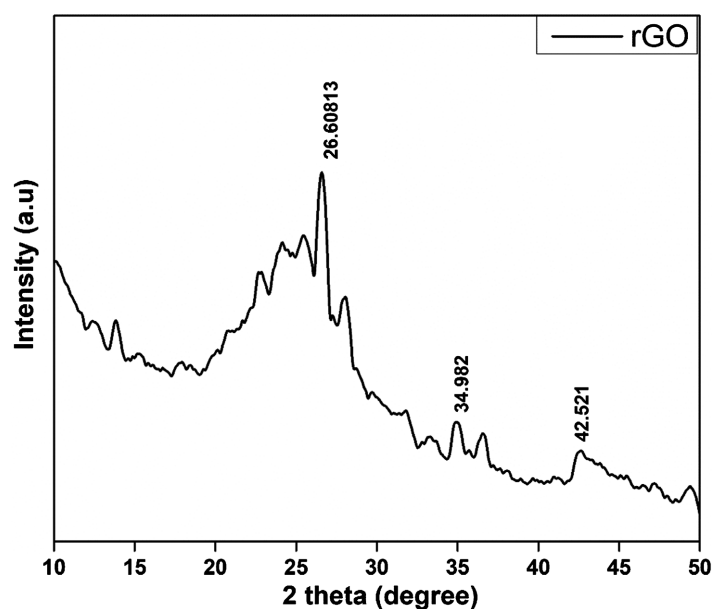
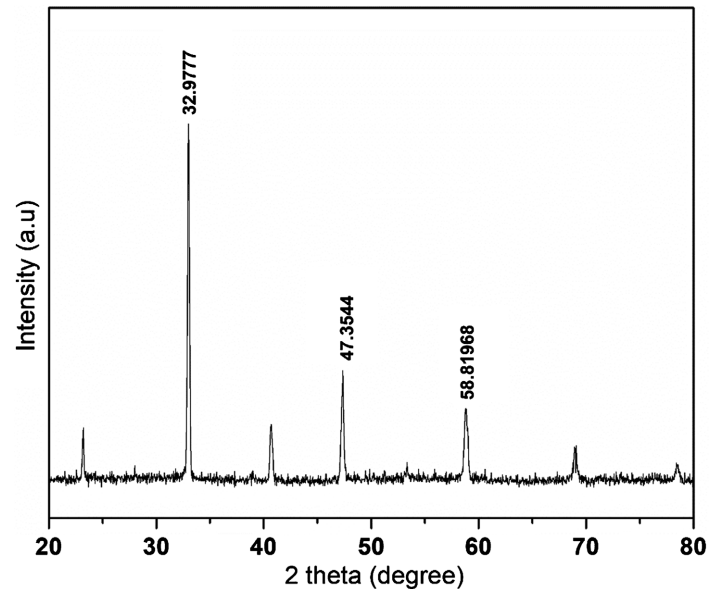


Figure 5. XRD analysis of rGO.

Table 2. Calculation of crystalline size of rGO by Scherrer's formula.

Peak position	FWHM	Crystallite size	Average size
26.60	0.6080	14.22	
34.98	1.3937	6.26	8.14 nm
42.52	2.267	3.94	

**Figure 6.** XRD analysis of NBT.**Table 3.** Calculation of crystalline size of NBT by Scherrer's formula.

Peak position	FWHW	Crystallite size	Average Crystallite size
32.98	0.21	41.22 nm	
47.34	0.28	32.37 nm	31.91 nm
58.81	0.43	22.16 nm	

of XRD results we can analysis the plane and peaks (**Figure 6**). The results show three peaks at different positions. The intensity of major peak is 32.98 (a.u) in these peaks two other peaks are NBT material are 47.34 and 58.81 (a.u) [34].

The crystalline size of NBT is calculated by the Scherrer's formula which is given in **Table 3**. The crystalline size at 32.98 (a.u) is 41.22 nm, where the size of crystalline at 47.34 and 58.81 (a.u) are 32.37 and 22.16 nm respectively. The average crystalline size of NBT is taken as 31.91 nm.

4. Conclusion

The conclusion of this research work is synthesis graphene oxide by graphite powder by using improved Hummer's method without using NaNO_3 . Without using NaNO_3 still produce same characteristic of GO. By the help of auto clave GO is thermally reduced to rGO after heating at 160°C for 6 hours. Taking so-

dium bismuth titanate powder (NBT) to prepare rGO/NBT composites, now use different weight percentage (1%, 3% & 5%) of rGO in NBT. The composites were synthesis by ball milling and pressing under 3 MPa pressure and sintered at 1075°C. FTIR results shows that different functional group attached with GO, rGO and composite of different concentration. Optical Microscopy images shows dispersion of rGO in NBT ceramic. With the help of LCR Meter, we measure decrease in electrical conductivity of composites (1%, 3%, 5%) at 200°C ($\sigma_{\text{NBT}} = 0.01005$, $\sigma_{1\%} = 0.00221$, $\sigma_{3\%} = -0.00179$, $\sigma_{5\%} = -0.00317$). By using XRD results calculate crystalline size of the sample by Scherrer's formula.

Conflicts of Interest

The authors declare no conflicts of interest regarding the publication of this paper.

References

- [1] Wang, C., Zhao, L., Liu, Y., Withers, R.L., Zhang, S. and Wang, Q. (2016) The Temperature-Dependent Piezoelectric and Electromechanical Properties of Cobalt-Modified Sodium Bismuth Titanate. *Ceramics International*, **42**, 4268-4273. <https://doi.org/10.1016/j.ceramint.2015.11.103>
- [2] Benyoussef, M., Zannen, M., Belhadi, J., Manoun, B. and Dellis, J. (2018) Dielectric, Ferroelectric, and Energy Storage Properties in Dysprosium Doped Sodium Bismuth Titanate Ceramics. *Ceramics International*, **44**, 19451-19460. <https://doi.org/10.1016/j.ceramint.2018.07.182>
- [3] Sangsubun, C. (2015) Fabrication and Characterization of Bismuth Sodium Titanate Ceramics by High-Energy Ball Milling Technique. *Ceramics International*, **41**, S180-S184. <https://doi.org/10.1016/j.ceramint.2015.03.123>
- [4] Shi, R., *et al.* (2019) Particle Transport Mode during Flash Sintering of Sodium Bismuth Titanate Ceramic. *Ceramics International*, **45**, 13269-13274. <https://doi.org/10.1016/j.ceramint.2019.04.015>
- [5] Reichmann, K., Feteira, A. and Li, M. (2015) Bismuth Sodium Titanate Based Materials for Piezoelectric Actuators. *Materials*, **8**, 8467-8495. <https://doi.org/10.3390/ma8125469>
- [6] Rao, C.N.R., Sood, A.K., Subrahmanyam, K.S. and Govindaraj, A. (2009) Graphene: The New Two-Dimensional Nanomaterial. *Angewandte Chemie*, **48**, 7752-7777. <https://doi.org/10.1002/anie.200901678>
- [7] Xia, K., Zhan, H. and Gu, Y. (2017) Graphene and Carbon Nanotube Hybrid Structure: A Review. *Procedia IUTAM*, **21**, 94-101. <https://doi.org/10.1016/j.piutam.2017.03.042>
- [8] Leggett, L.A.J. (2010) Lecture 5: Graphene: Electronic Band Structure and Dirac Fermions. 1-12.
- [9] Qin, H., Sun, Y., Zhe, J. and Liu, Y. (2010) Mechanical Properties of Wrinkled Graphene Generated by Topological Defects. *Carbon*, **108**, 204-214. <https://doi.org/10.1016/j.carbon.2016.07.014>
- [10] Shevitski, B. (2010) Structural Properties of Graphene and Carbon Nanotubes. University of California Los Angeles, Los Angeles, CA.
- [11] Moon, P. and Koshino, M. (2013) Optical Absorption in Twisted Bilayer Graphene.

- Physical Review B*, **87**, Article ID: 205404.
<https://doi.org/10.1103/PhysRevB.87.205404>
- [12] Rozhkov, A.V., et al. (2011) Electronic Properties of Mesoscopic Graphene Structures: Charge Confinement and Control of Spin and Charge Transport. *Physics Reports*, **503**, 77-114.
- [13] Jaiswal, M. (2017) Graphene: A Review of Optical Properties and Photonic Applications. *Asian Journal of Physics*, **25**, 809-831.
- [14] Zaaba, N.I., Foo, K.L., Hashim, U., Tan, S.J., Liu, W. and Voon, C.H. (2017) Synthesis of Graphene Oxide Using Modified Hummers Method: Solvent Influence. *Procedia Engineering*, **184**, 469-477. <https://doi.org/10.1016/j.proeng.2017.04.118>
- [15] Journal, I., Energy, R. and Issn, E.E. (2014) Graphene Oxide Synthesized by Using Modified Hummers Approach. *International Journal of Renewable Energy and Environmental Engineering*, **2**, 58-63.
- [16] Chen, J., Yao, B., Li, C. and Shi, G. (2013) An Improved Hummers Method for Eco-Friendly Synthesis of Graphene Oxide. *Carbon*, **64**, 225-229.
<https://doi.org/10.1016/j.carbon.2013.07.055>
- [17] Pei, S. and Cheng, H.M. (2012) The Reduction of Graphene Oxide. *Carbon*, **50**, 3210-3228. <https://doi.org/10.1016/j.carbon.2011.11.010>
- [18] Ghorbani, M., Abdizadeh, H. and Golobostanfard, M.R. (2015) Reduction of Graphene Oxide via Modified Hydrothermal Method. *Procedia Materials Science*, **11**, 326-330. <https://doi.org/10.1016/j.mspro.2015.11.104>
- [19] Shi, J., Du, W., Yin, Y., Guo, Y. and Wan, L. (2014) Hydrothermal Reduction of Three-Dimensional Graphene Oxide for Binder-Free Flexible Supercapacitors. *Journal of Materials Chemistry A*, **2**, 1-10. <https://doi.org/10.1039/c4ta01547a>
- [20] Porwal, H., Grasso, S. and Reece, M.J. (2013) Review of Graphene-Ceramic Matrix Composites. *Advances in Applied Ceramics*, **112**, 443-454.
<https://doi.org/10.1179/174367613X13764308970581>
- [21] Phiri, J., Gane, P. and Maloney, T.C. (2017) General Overview of Graphene: Production, Properties and Application in Polymer Composites. *Materials Science and Engineering: B*, **215**, 9-28. <https://doi.org/10.1016/j.mseb.2016.10.004>
- [22] Liu, J., Yan, H. and Jiang, K. (2013) Mechanical Properties of Graphene Platelet-Reinforced Alumina Ceramic Composites. *Ceramics International*, **39**, 6215-6221.
<https://doi.org/10.1016/j.ceramint.2013.01.041>
- [23] Walker, L.S., Marotto, V., et al. (2011) Toughening in Graphene Ceramic Composites. *ACS Nano*, **5**, 3182-3190. <https://doi.org/10.1021/nn200319d>
- [24] Miranzo, P., Belmonte, M. and Osendi, M.I. (2017) From Bulk to Cellular Structures: A Review on Ceramic/Graphene Filler Composites. *Journal of the European Ceramic Society*, **37**, 3649-3672. <https://doi.org/10.1016/j.jeurceramsoc.2017.03.016>
- [25] Huang, H., Tang, J. and Liu, J. (2019) Preparation of Na_{0.5}Bi_{0.5}TiO₃ Ceramics by Hydrothermal-Assisted Cold Sintering. *Ceramics International*, **45**, 6753-6758.
<https://doi.org/10.1016/j.ceramint.2018.12.166>
- [26] Petrus, M., Wozniak, J., Cygan, T., Adamczyk-Cieslak, B. Kostecki, M. and Olszyna, A. (2017) Sintering Behaviour of Silicon Carbide Matrix Composites Reinforced with Multilayer Graphene. *Ceramics International*, **43**, 5007-5013.
<https://doi.org/10.1016/j.ceramint.2017.01.010>
- [27] Alam, S.N., Sharma, N. and Kumar, L. (2017) Synthesis of Graphene Oxide (GO) by Modified Hummers Method and Its Thermal Reduction to Obtain Reduced Graphene Oxide (rGO). *Graphene*, **6**, 1-18.

- <https://doi.org/10.4236/graphene.2017.61001>
- [28] Zaaba, N.I., Foo, K.L., Hashim, U., Tan, S.J., Liu, W.W. and Voon, C.H. (2017) Synthesis of Graphene Oxide Using Modified Hummers Method: Solvent Influence. *Procedia Engineering*, **184**, 469-477. <https://doi.org/10.1016/j.proeng.2017.04.118>
- [29] Porwal, H. (2015) Processing and Properties of Graphene Reinforced Glass/Ceramic Composites. Queen Mary University of London, London.
- [30] Falkovsky, L.A. (2008) Optical Properties of Graphene. *Journal of Physics: Conference Series*, **129**, Article ID: 012004.
- [31] Silvestre, J., Silvestre, N. and De Brito, J. (2015) An Overview on the Improvement of Mechanical Properties of Ceramics Nanocomposites. *Journal of Nanomaterials*, **2015**, Article ID: 106494. <https://doi.org/10.1155/2015/106494>
- [32] Muñoz-Ferreiro, C., *et al.* (2019) Microstructure, Interfaces and Properties of 3YTZP Ceramic Composites with 10 and 20 vol% Different Graphene-Based Nanostructures as Fillers. *Journal of Alloys and Compounds*, **777**, 213-224. <https://doi.org/10.1016/j.jallcom.2018.10.336>
- [33] Zeller, F., Müller, C., Miranzo, P. and Belmonte, M. (2017) Exceptional Micromachining Performance of Silicon Carbide Ceramics by Adding Graphene Nanoplatelets. *Journal of the European Ceramic Society*, **37**, 3813-3821. <https://doi.org/10.1016/j.jeurceramsoc.2017.03.072>
- [34] Ayrikyan, A., *et al.* (2018) Investigation of Residual Stress in Lead-Free BNT-Based Ceramic/Ceramic Composites. *Acta Materialia*, **148**, 432-441. <https://doi.org/10.1016/j.actamat.2018.02.014>